Benjamin Schmidt-Hansberg (Autor)

Process-structure-property relationship of polymer-fullerene bulk heterojunction films for organic solar cells

Drying process, film structure and optoelectronic properties

https://cuvillier.de/de/shop/publications/29

1 Introduction

Photovoltaic (PV) is attracting increasing interest as an important contribution to renewable energy supply. This trend is getting strengthened by increasing price of fossil fuels, concerns over vast amounts of green house gases and upcoming discussions about the back out of the nuclear energy supply. In 2009, the world consumed in total 11164.3 million tons oil equivalent of fossil fuels corresponding to about 4.675×10^{20} J of primary energy consumption. [1] The total annual solar energy available to the earth is approximately 3.9×10^{24} J/a which is equivalent to 1.08×10^{18} kWh [2] with a global mean of about 170 W/m² [3]. This is more than 8000 times the world primary energy consumption. So if harnessed properly, solar energy can be used to cover the global energy needs. Presently, commercially dominating photovoltaic modules are based on crystalline silicon (first generation PV) or thin film techniques (second generation PV) as for instance copper indium gallium selenide (CIGS) or cadmium telluride (CdTe) solar cells. Silicon solar cells require energetically intensive high temperature processes, which leads to energy payback times in the range of 2-5 years [4-6]. On the other hand thin film solar cells like CIGS and CdTe can be fabricated more efficiently by vapor deposition, which reduces the energy payback time to about 1 year for CdTe. However, such thin film solar cells commonly require processing under high vacuum which still demands high needs of energy if the vapor deposition rates limit the fabrication throughput. Particle based printing processes and evaporation under ambient conditions are therefore under development for thin film PV.

In addition to the mentioned inorganic PV technologies organic photovoltaics (third generation PV) could make solar energy more affordable with energy payback times potentially in the order of months or weeks. No high temperature or high vacuum processes are required and the fabrication process can be conducted in a large area, so called roll-to-roll (R2R) coating process, from solution. Solution processing is an intrinsic advantage of soluble organic semiconductors[1]. The mechanical flexibility of the active

[1] In 2000 A.J. Heeger, A.G. MacDiarmid and H. Shirakawa received the Nobel Prize for Chemistry "for their discovery and development of conductive polymers".

layer with thicknesses below 500 nm allows for the realization of flexible [7-10], stretchable [11] or solar cells on paper [12] or as textile fibers [13, 14]. Although light weight and mechanical flexibility offers many interesting applications for organic photovoltaic (OPV) their efficiency is not yet competitive with the inorganic counterparts. Table 1.1 depicts the current state of some exemplary photovoltaic technologies.

Table 1.1: Selected record efficiencies for different organic and inorganic solar cell devices [15, 16].

Classification	Efficiency	Test Center (Date)	Manufacturer
Organic polymer	8.3%	NREL (11/10)	Konarka
Organic (tandem)	8.3%	FhG-ISE (10/10)	Heliatek
Dye sensitized	10.4%	AIST (08/05)	Sharp
Silicon (crystalline)	25%	Sandia (03/99)	UNSW PERL
Silicon (multicryst.)	20.4%	NREL (05/04)	FhG-ISE
Silicon (amorphous)	10.1%	NREL (07/09)	Oerlikon Solar Lab
GaAs (thin film)	27.6%	NREL (11/10)	Alta Devices
CIGS	20.3%	FhG-ISE (08/10)	ZSW
CdTe	16.7%	NREL (09/01)	NREL

However, the advantage of OPV is the considerable reduction of fabrication costs which would make this technology competitive even at PCE below those of inorganic solar cells. Reduced fabrication costs of the solution cast layers of the OSC can be reached by large area coating and printing processes. For this purpose different coating techniques like knife over roll [17], slot die [17-20], screen printing [10, 17-19, 21, 22] and gravure coating [18, 23] have been proven to be suitable for large area fabrication of organic solar cells (OSC). Further large area deposition techniques are spray coating [24-28] and ink-jet printing [29, 30]

Recently, Krebs et al. have evaluated the cost of their R2R fabricated OSC to be 89 €/m² and 8.1 €/W_p [19], where the latter depicts the costs per generated electric power at standardized 1000 W/m² illumination and Air Mass 1.5 (AM 1.5) light spectrum. Even though the cost in €/W_p is comparable to the cost for electricity using existing technologies the levelized cost of

electricity (LCOE) is expected to be significantly higher than the existing technologies due to the inferior operational lifetime. Currently available OPV devices are thus competitive for consumer electronics but ill-suited for on-grid electricity production [19]. Dennler et al. estimated that OPV can become competitive at 7% efficiency and a lifetime of 7 years [31]. Although the maximum power conversion efficiency shows a fast progress and has reached presently a record efficiency of 9.2% at laboratory scale [32], many details from physical fundamentals up to the influence of the fabrication process on the device properties remain unclear. This thesis focuses therefore upon the fabrication process-device property relationship in order to facilitate the transfer from laboratory results to large scale manufacturing.

1.1 Principles of organic solar cells

In photovoltaic devices sunlight is absorbed in the photoactive layer, which excites electrons. Subsequently electrons and defect electrons, so called holes, are separated and collected at the electrodes. By this process a voltage in-between both electrodes is generated, which serves as power source.

In inorganic photovoltaic devices thermal energy at room temperature is sufficient for the dissociation of the photo-induced electron-hole pair within a single material (homojunction). In contrast to inorganic PV, organic semiconductors exhibit higher binding energies of the electron-hole-pair, also called exciton [33] which requires the incorporation of a second material in a so called heterojunction [34]. In this concept two materials with differing HOMO and LUMO energy levels are brought into contact with each other (Figure 1.1).

If electrons are excited at the light absorbing electron donator by photon absorption from the HOMO to the LUMO level, they leave a positive charge (hole) at the HOMO. Subsequently the excitons have to diffuse within the electron donating material to the interface with the electron accepting material. The diffusion distance is limited by the exciton lifetime to about 5-10 nm before recombination [35-37]. At the donator-acceptor interface the lower LUMO energy level of the electron acceptor is energetically preferred. If the LUMO-LUMO energy level difference exceeds the electron-hole binding energy, the charge carriers can be separated at the interface. LUMO positions of the polymer and acceptor separated by roughly 0.3 eV are expected to yield satisfactory charge separation and prevent charge recombination. [38-40]

Subsequently, the charges travel within the appropriate phases to the electrodes: holes within the electron donator phase (here polymer) and electrons within the electron acceptor phase (here fullerene). The theoretical voltage maximum of the solar cell device at open-circuit conditions (no current) V_{oc} can be determined from the difference of $LUMO_{acceptor}$-$HOMO_{donor}$.

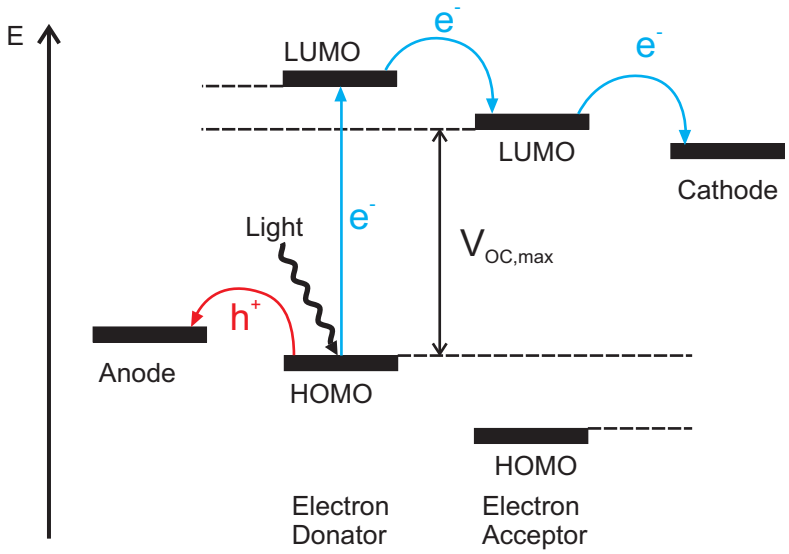

Figure 1.1: Energy level scheme of the steps of exciton generation, diffusion, dissociation and charge transport to the electrodes within each phase for the heterojunction concept. (According to [38])

For efficient solar cells it is worthwhile to generate short diffusion paths to the donator-acceptor interface, because of the very limited exciton diffusion length. Another important fact is the correlation of the amount of separated excitons with the donator-acceptor interface area, which should be as high as possible. Short exciton diffusion paths and an increased donator-acceptor interface can be achieved by the mixture of both phases. Figure 1.2 depicts a simplified scheme of the intermixed donator-acceptor structure of the bulk heterojunction (BHJ) concept [41, 42] and the typical architecture of a polymer solar cell. The challenge of the BHJ structure is to optimize the maximized interface area on the one hand, by providing sufficient interpenetrating charge transport pathways to the electrodes [43]. Charges that are generated at isolated domains remain trapped and cannot contribute to solar energy harvesting. It should be mentioned, that the image of clearly separated pure phases does not reflect the real character of interpenetrating morphology [44]. Additionally the crystallinity and the orientation of crystallites within the phases are of importance for the charge carrier mobility [45-47]. The solar

cell architecture comprises a transparent indium tin oxide (ITO) anode on top of the substrate (glass slides or plastic foils), followed by the solution processed hole conductive layer Poly(3,4-ethylendioxythiophene): Poly(styrenesulfonate) (PEDOT:PSS) and the active layer (here P3HT:PCBM). On top of the active layer it is common to deposit a calcium/aluminum cathode[1] by evaporation through a shadow mask.

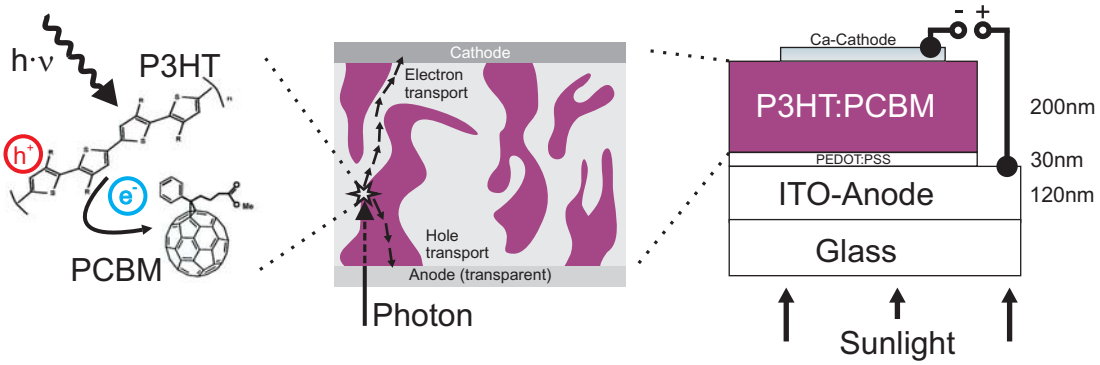

Figure 1.2: Structure of the polymer solar cell with approximate film thicknesses. Electron donor (P3HT) and acceptor (PCBM) are blended together to maximize the interface area where exciton dissociation into electrons and holes takes place. For an efficient photocurrent, each material must provide a continuous path for electron and hole transport to the respective contact. Isolated domains can collect charges and cause recombination.

For the electrical description of organic photovoltaics, the two-diode-model is suitable [48]. The equivalent circuit scheme of this model is shown in Figure 1.3, where I_{sc} is the generated photocurrent, D_1 the diode that determines the dark current and D_2 represents recombination losses. R_S and R_P represent the series and parallel resistance.

[1] For large area coating applications the moisture and oxygen sensitive calcium layer has to be replaced [10, 263, 264][265].

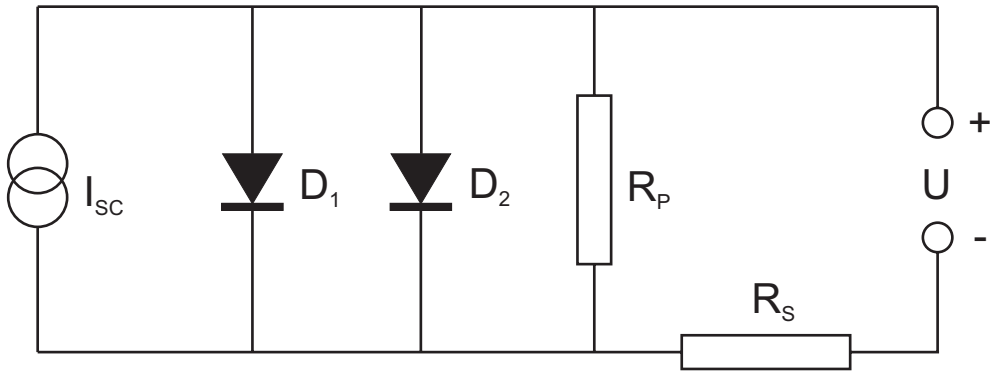

Figure 1.3: Equivalent circuit scheme of an organic solar cell.

The current density-voltage characteristics (JV-characteristics) describe the behavior of an organic solar cell and can be related to parameters of the equivalent circuit. The JV-curve of a solar cell corresponds basically to the characteristics of a diode shifted about the amount of the photocurrent (Figure 1.4a). This is the case if the resistances and recombination losses are independent from illumination of the device. The point at the JV-curve where the generated power ($P = V \cdot I$) reaches a maximum is called maximum power point (MPP). The highest voltage at the solar cell is reached at open-circuit conditions ($I = 0$) and is denoted as V_{oc} or U_{oc}. The highest current is reached under short-circuit conditions ($V = 0$) and denoted as I_{sc} or as J_{sc} for the area related current density. The power conversion efficiency η (PCE) of a solar cell is determined by the ratio of generated electric power to the incident light power.

$$\eta = \frac{V_{MPP} \cdot I_{MPP}}{P_{light}} = \frac{V_{oc} \cdot I_{sc} \cdot FF}{P_{light}} \qquad 1.1$$

The fill factor *FF* describes the ratio between the power at MPP and the product of V_{oc} and I_{sc}.

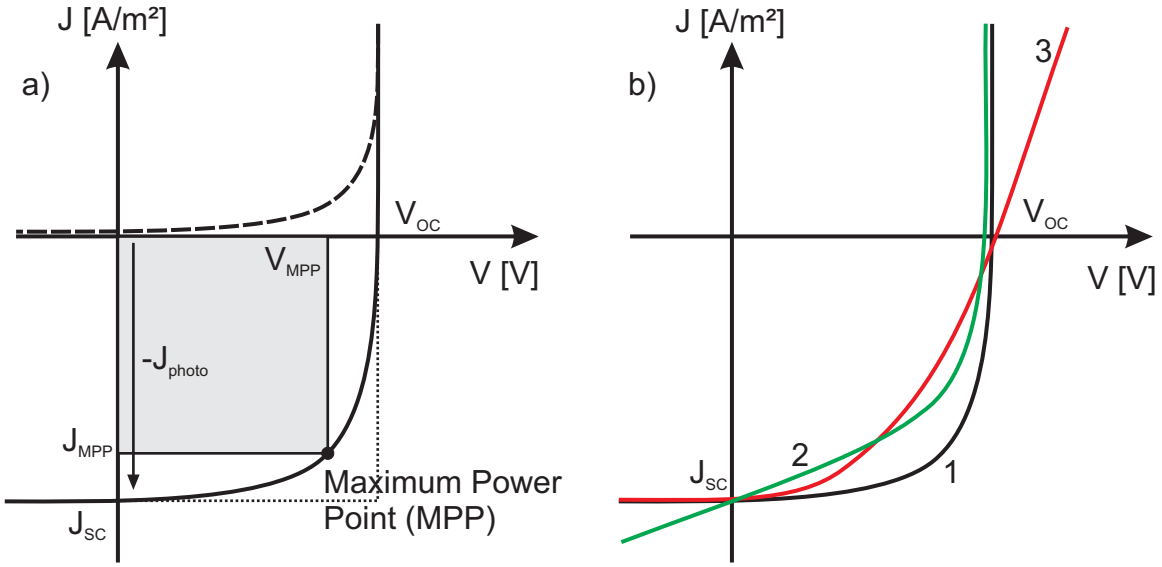

Figure 1.4: a) Current density-voltage (JV) characteristics of a solar cell. Dark curve (dashed line) and under illumination (solid line). b) JV-characteristics for an "ideal" solar cell (1) with negligible series resistance and almost infinite parallel resistance. Case (2) exhibits a finite parallel resistance and case (3) an increased series resistance. [49]

The series and parallel resistance are important for the performance of solar cells. An ideal solar cell exhibits an infinite parallel resistance and a negligible series resistance (case 1 in Figure 1.4b). This ideal case is usually not reached. The parallel resistance is proportional to the reciprocal slope of the JV-curve for $V \leq 0$ before the diode breaks through. Decreasing parallel resistance is expressed by an increasing slope in forward regime at high voltage (case 2 in Figure 1.4b). The series resistance can be derived from the reciprocal slope at comparatively high voltages, since it is the determining parameter in that range. An increased series resistance is expressed by a decreasing slope at V_{oc} (case 3 in Figure 1.4b).

1.2 Organic semiconductors

For the investigation of the impact of fabrication scenarios on the solar cell properties of organic solar cells, the well-established electron donating polymer poly-(3-hexylthiophene) (P3HT, Figure 1.5) was mainly investigated in this thesis. The transferability of the observed mechanisms and correlations as obtained for P3HT was accomplished for the low band gap polymers poly{[4,4-bis(2-ethylhexyl)-cyclopenta-(2,1-b;3,4-b')dithiophene]-2,6-diyl-

alt-(2,1,3- benzothiadiazole)-4,7-diyl} (PCPDTBT, Figure 1.5) and the similar polymer containing a silicon bridging atom poly{[4,40-bis(2-ethylhexyl)dithieno(3,2-b;20,30-d)silole]-2,6-diyl-alt-(2,1,3-benzothidiazole)-4,7-diyl} (PSBTBT[1], Figure 1.5).

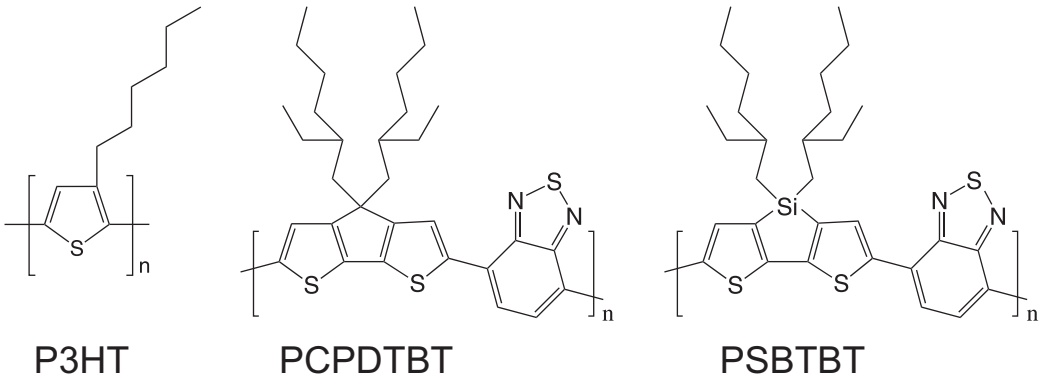

Figure 1.5: Structures of the investigated electron donating polymers.

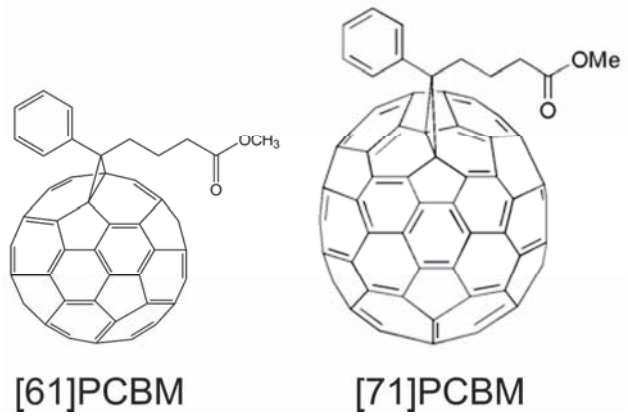

Figure 1.6: Structures of the investigated electron accepting fullerene derivatives. [50]

In the photoactive layer, these electron donating polymers are combined with electron accepting fullerene[2] derivatives like [6,6]-phenyl C61-butyric acid methyl ester ($PC_{61}BM$, Figure 1.6) and [6,6]-Phenyl C71-butyric acid methyl ester ($PC_{71}BM$, Figure 1.6). Reasons for the incorporation of these two

[1] In literature the abbreviation Si-PCPDTBT is also common.
[2] Harold Kroto, Robert Curl and Richard Smalley were awarded the 1996 Nobel Prize in Chemistry for their roles in the discovery of buckminsterfullerene and the related class of molecules, the fullerenes.

types of materials and the concept of organic solar cells shall be explained below in section 1.1

One property which all organic semiconductors have in common is the conjugated π-electron system, i.e. alternating single and double bonds, along the entire molecule of the organic semiconductor. In this configuration all carbon atoms exhibit a sp^2-hybridization state. While the three sp^2-orbitals are ordered planar as indicated in Figure 1.7 (right), the unhybridized p_z-orbital stands normal to the sp^2-orbital plane. Within the sp^2-orbital plane, single bonds (σ-bonds) are formed. Overlapping p_z-orbitals of neighboring carbon atoms can additionally form a weaker π-bond, which leads in sum to a double bond. For the case of alternating single and double bonds, p_z-orbitals can either overlap with one or the other neighboring carbon atom which is a dynamically changing process. In time average this leads to the delocalization of π-electrons in one large π-orbital over the entire conjugated electron system. This interaction of p_z-orbitals within one molecule leads to the formation of a multitude of possible electronic states. In the non-excited ground state electrons will occupy energetically favorable states, which is the Highest Occupied Molecular Orbital (HOMO). This molecular orbital is the analogue of the valence band in inorganic semiconductors. The Lowest Unoccupied Molecular Orbital (LUMO) represents the analogue of the conductive band in inorganic semiconductors.

In this work polymers are used as hole conducting (p-type) electron donating materials and fullerene derivatives as electron accepting and conducting (n-type) compounds. Figure 1.7a exemplarily depicts the unit cell of the hole (h^+) conducting polymer P3HT, which exhibits a conjugated electron system along the polymer backbone. Hence, charges can travel along the polymer backbone within the plane of sp^2-orbitals due to overlapping p_z-orbitals.

The charge transport from one polymer backbone to the other, where the distance of the hexyl-side chains must be overcome is not possible, since the side chains are not part of the conjugated electron system [51]. Because p_z-orbitals protrude out of the plane of σ-bonds which are formed by sp^2-orbitals (indicated as grey planes in Figure 1.7), polymers tend to stack in a manner such that p_z-orbitals additionally overlap in the (020) stacking direction according to the crystallographic nomenclature. This effect is called π-π-stacking and it provides additional charge transportation in p_z-orbital direction normal to the plane of σ-bonds.

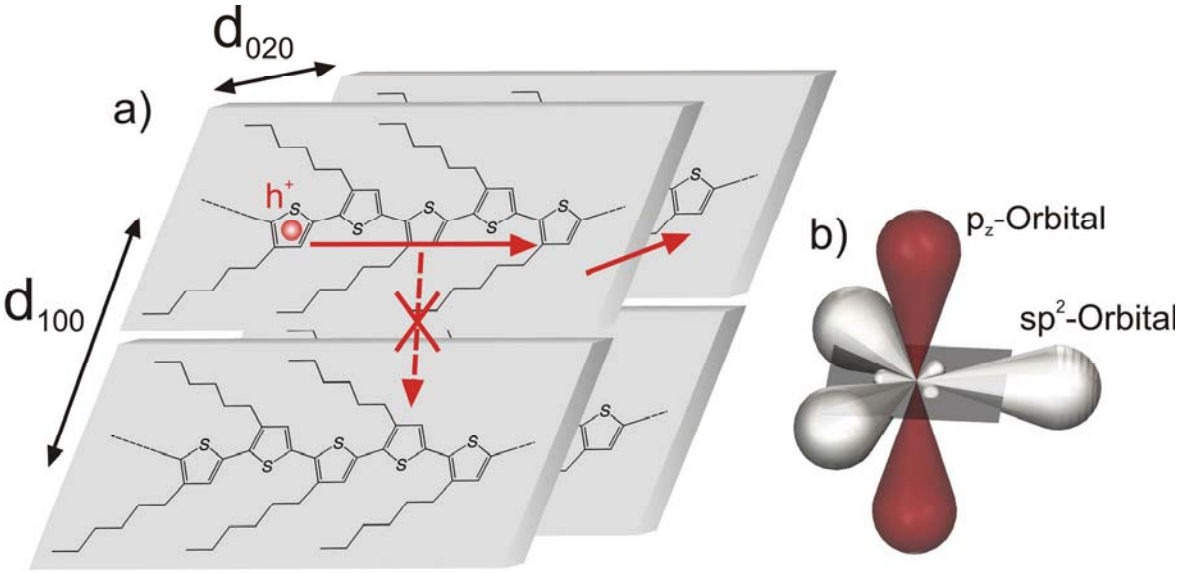

Figure 1.7: a) Scheme of hole (h+) transport in P3HT along the polymer backbone and in π-π-stacking direction indicated by red arrows. The spacing in intra layer (100) and inter layer (020) π-π-stacking are denoted as d_{100} and d_{020} respectively. b) Drawing of sp^2-hybredized orbitals.

The average chain length of P3HT investigated in this thesis ($M_w \approx 40.000 – 60.000$ g/mol, polydispersity ≈ 1.7-1.9) is in the order of several hundred thiophene units. The effective conjugation length of polythiophene, which is the length of continuously delocalized π-electron system along the polymer backbone, is typically in the range of ≈ 10 thiophene units [52, 53]. Reasons for the low conjugation length can be distorted polymers and kinks along the backbone [54]. These barriers must be overcome by so called hopping processes of the charge carriers. In amorphous materials hopping processes are the dominating charge transport mechanism, which usually leads to lower charge carrier mobility in comparison to semi-crystalline materials.

1.3 Morphology of polymer-fullerene blends

The performance of organic solar cells strongly depends on the phase separated polymer-fullerene structure which forms by self assembly during the solvent evaporation step subsequent to the coating process [55-58] and can further be modified by post process treatments, such as thermal [59-63] or solvent annealing [64-66]. Domain sizes, degree of crystallinity, molecular orientation and the interpenetrating network geometry are important morpho-

logical parameters for the optimization of solar cell performance. Several review articles discuss the crucial importance of morphology for the efficiency of OPV and demand an improved understanding of the driving assembly mechanisms [67-70]. Due to the paramount relevancy of this topic it has been of great research interest worldwide over the past years. The knowledge about morphology and its relation to the physical properties of solar cells are still under progress.

At the beginning of this thesis the image of morphology was basically a three dimensional phase separated structure of pure donor and acceptor domains. Since the structures are very small (desired in the range of a few tens of nanometers) and the optical contrast is very low for the predominantly carbon containing materials, it has been very challenging to obtain reliable images of the film structure by common microscopy methods. This section gives a brief overview about common methods for the structural investigation of BHJ blends. Several review articles give a broader overview of appropriate experimental techniques [51, 71-73]. Morphology aspects are discussed in more detail in chapter 4 in conjunction with results obtained in this work, which contributed to an improved and more detailed image of the polymer-fullerene blend structure. In the following, the presently most relevant techniques and reported results are exemplarily discussed with some selected publications.

Molecular scale: X-ray diffraction and scattering X-ray techniques are in general suitable for the investigation of crystalline structures. For the determination of crystallographic structures in thin films they are commonly operated at very low angles of the incident beam close to total reflection in the order of 0.1-0.2 degree, which is called grazing incidence [74]. Grazing incidence X-ray diffraction (GIXD) or similar techniques have been used in numerous publications for the determination of the crystalline polymer structure and their orientation with respect to the substrate [75, 76]. Recent works exploited the advantage of bright synchrotron[1] based X-ray sources for in-situ measurements during thermal [63, 77, 78] or solvent annealing [79]. By changing the angle of incidence it is even possible to adjust the penetra-

[1] A synchrotron is a type of cyclic particle accelerator in which the magnetic field and the electric field (to accelerate the particles) are synchronized with the travelling particle beam.

tion depth of the X-ray beam and probe the structure vertically resolved. In this work GIXD could be applied for the first time for monitoring the molecular ordering of polymer-fullerene blends during film drying in real time [58, 80, 81], which is explained in more detail in section 4.2.1. This technique provides quantitative information on polymer chain spacing, their orientation with respect to the substrate, domain size (correlation length) and the relative amount of crystallites (related to signal intensity). The detectable structure scale ranges from the molecular scale to the size of crystalline domains.

Cluster and domain scale: Neutron scattering Kiel et al. demonstrated by the application of small angle neutron scattering (SANS) at polymer-fullerene blend films that small scale crystallites form superior aggregate structures [82, 83]. Thermal annealing leads to increasing PCBM cluster sizes. This method is very useful, since it covers the intermediate structural scale between X-ray and electron microscopy techniques.

Domain and topography scale: Electron microscopy Typical electron microscopic methods for transmission measurements are transmission electron microscopy (TEM), scanning transmission microscopy (STEM) [84, 85] and selected area electron diffraction (SAED). While TEM is sensitive to the local density of the sample, STEM can provide higher sensitivity to material contrast, i.e. the atomic number, if operated with a high-angle annular dark-field (HAADF) detector. SAED diffraction patterns give information about the crystallographic film structure.

The difficulty of TEM measurements at BHJ layers [60, 86-88] is the low contrast between both mainly carbon containing materials and the small structure scale of a few tens of nanometers. A trick is to slightly defocus the microscope. Excessive defocusing falsifies the structure scale. 50-100 nm thin films must be prepared, in order to prevent shadow effects. The smoothness of the film is important, since high roughness causes additional contrast due to lateral deviations in electron penetration length through the sample. Usually the BHJ film is lifted off the water soluble PEDOT:PSS layer and is transferred to a common TEM copper grid. This device destructive, but not film destructive procedure is the same for all measurements mentioned in this section that are operated in transmission. If used properly, TEM can reveal the fibril structure of P3HT in the BHJ blend and also depicts the larger scale film

topography [60]. The dimensions of such P3HT whiskers are about 3-7 nm in height, 15 nm in width and about 0.2-5 μm in length [45, 89]. A more comprehensive image of the three dimensional (3D) morphology can be obtained by electron tomography [66, 85, 90]. This is basically done by a series of TEM measurements at different angles of incident (i.e. from +70° to -70°). It should be noted that the image contrast of this technique originates mainly from the density difference of crystalline and amorphous regions. Polymer and fullerene phases can hardly be deciphered. These structural 3D measurements furthermore deliver information of the vertical distribution of crystalline volume fraction.

Vertical gradients The vertical donor-acceptor ratio is crucial for charge carrier transport, since electrons are collected at the top electrode and holes at the bottom electrode in regular device architecture. Hence, polymer enrichment close to the top electrode would cause a barrier for electron extraction. A method that is very sensitive to vertical gradients in BHJ layers is neutron reflectivity [82, 91, 92]. The difference in scattering length density (SLD) of P3HT ($0.80 \pm 0.01 \times 10^{-6}$ Å^{-2}) and PCBM (4.34×10^{-6} Å^{-2}) provides sufficient contrast between both materials [92]. The vertical gradient is determined indirectly by model fits to the reflectivity measurements where the angle of incident is scanned. Another way for the determination of the vertical gradient is variable angle spectroscopic ellipsometry (VASE). In VASE, changes in the polarization state are utilized for model fits of the complex refractive index of the investigated film, which can also provide vertical information [93, 94]. A destructive method for the determination of vertical concentration gradients is secondary ion mass spectrometry (SIMS) [95-98]. Here the film is sputtered with typically Ga^+ ions and subsequently analyzed by mass spectrometry. A critical issue is the sputtering rate, which might be very different for multi component systems. Another possibility to investigate the vertical gradient is to lift off the BHJ layer and measure the chemical composition on the top and bottom surface of the film with surface sensitive techniques.

Surface sensitive techniques X-ray photoelectron spectroscopy (XPS) is capable of measuring the chemical composition at surfaces. An incident X-ray beam generates photoelectrons close to the surface which are detected with respect to their kinetic energy and intensity. This results in spectra that are

characteristic for a distinct composition. After initial pure substance calibration XPS allows for a quantitative determination of the chemical composition at the surface. Due to the short mean free path of the photoelectrons, the probing depth of XPS is only 6–8 nm [99]. XPS could be exploited for the comparison of the composition at the top and bottom interface of the BHJ layer [53, 100, 101]. In combination with ion sputtering it is used to investigate depth profiles in bulk materials and buried interfaces. Another technique for the determination of the surface composition is near-edge X-ray absorption fine structure spectroscopy (NEXAFS) which is more sensitive to structural features than XPS [71]. With NEXAFS, composition specific spectra are utilized for concentration determination [94, 102, 103]. Germack et al. measured the chemical composition at the bottom and top interface of the BHJ layer with NEXAFS and could proof the influence of substrate surface energy on the vertical polymer-fullerene-ratio gradient [102].

Another class of surface sensitive techniques is scanning probe microscopy (SPM) [72] whereby atomic force microscopy (AFM) [104] is the prevalent method. In AFM, the sample surface is scanned with a sharp tip providing mainly the surface topography and a sort of mechanical property mapping which is explained in more detail in section A 3.2.

Lateral chemical mapping In combination with scanning transmission X-ray microscopy (STXM) NEXAFS has been shown to be very utile for lateral chemical mapping when operated in transmission [44, 71, 105-107]. In this combined method the sample is first of all scanned by STXM for the identification of structures revealed by lateral contrast. Subsequently these lateral contrast features are investigated by NEFAXS analysis which provides the chemical composition after prior calibration and structure information with a spatial resolution of about 20-50 nm [71, 105]. If operated with polarized X-rays the polymer backbone or crystalline plane orientation can be determined according to interactions between the X-ray electric field and the delocalized electrons along the delocalized π-electron system [108].

1.4 Aim of this work

This work was encouraged by the observation of the drying process influence on the light absorption behavior of the photoactive layer of OSC. Initial drying experiments have been conducted in collaboration with Hung Do and Alexander Colsmann of the Light Technology Institute (LTI, Karlsruhe). This observation was supported by Li et al. [109] and Mihailetchi et al. [110] who demonstrated that the drying process of the photoactive layer in OPV devices influences the solar cell performance. This led to the hypothesis, that the drying process can be utilized for a systematic optimization of solar cell performance due to systematically induced morphological changes in the photoactive layer. The evaluation of the hypothesis requires the elaboration and investigation of different topics:

- Drying kinetics (evolution of thickness or composition) measurement and simulation of µm to nm thin multi component films
- Phase diagrams of organic semiconductor solutions
- Determination of driving mechanisms for film morphology
- Exploitation of the process-structure-property relationship in order to realize an optimized fabrication of solar cells (higher efficiency and faster production)

For the exploitation of the drying process in order to generate a favorable film structure it is mandatory to be able to describe the drying kinetics of the solution cast film. Therefore, new methods for the measurement of film drying kinetics from several micrometers to the nanometer scale have to be developed. This requires the elaboration of an experimental setup which allows for an accurate coating of wet film thicknesses below 10 µm combined with well-defined and reproducible drying conditions to obtain dry film thicknesses of 20-300 nm. In combination with this experimental setup a technique for the measurement of the drying kinetics of such thin films shall be elaborated.

In the theoretical part of this thesis, an appropriate model shall be developed, which is capable to describe the drying kinetics of such thin films for single and multiple solvent systems. This part can be conducted in continuation to previous work on film drying [111] and mass transport in polymeric membranes [112] which show many similarities. The validation shall be conducted with experimental data obtained from solution cast blends of organic semiconductors.

In the morphology and optoelectronic part of this thesis, the governing mechanisms of molecular ordering and their influencing parameters are the mayor interest. For a systematic exploitation of the self-assembly mechanisms their influencing parameters shall be explored. This requires new experimental approaches for in situ observations of the assembly process during film drying. A simultaneous measurement of the evolving film structure and film composition is required for this purpose.

The influence of drying time on solar cell device performance is expected to originate from differences in molecular assembly time induced by crossing solubility limits or entering thermodynamically unstable states. This assumption demands the comparative investigation of two competitive mechanisms: thermodynamic equilibrium and film formation kinetics. This requires on the one hand the determination of the solutions phase diagram (Figure 1.8a), which depicts the preferred thermodynamically equilibrium state at a distinct composition. On the other hand film drying kinetics (Figure 1.8b) can hinder that this state is reached, if kinetic limitation is given.

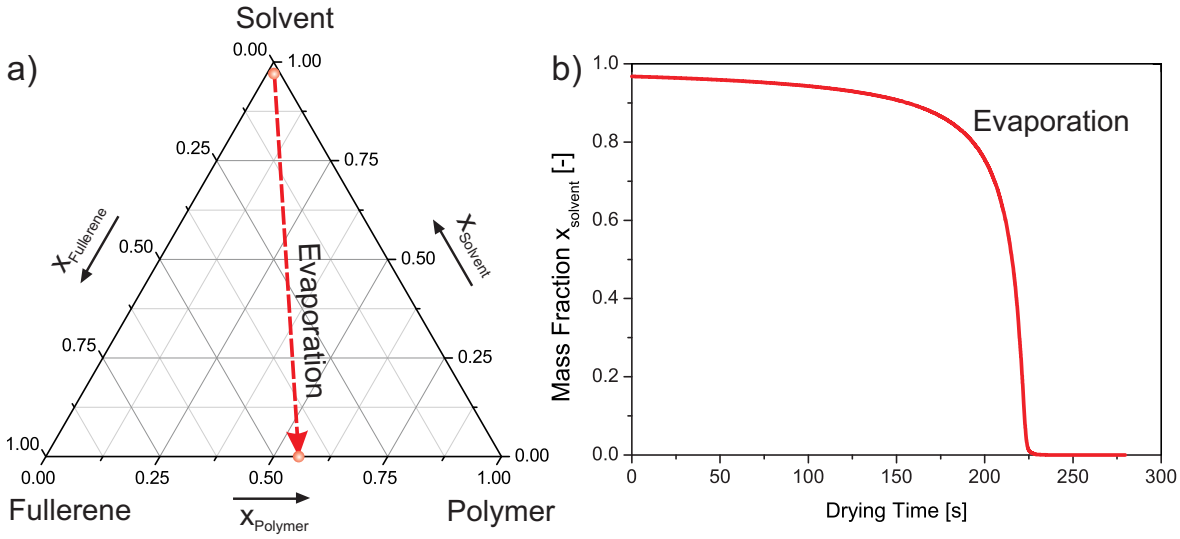

Figure 1.8: a) Schematic ternary phase diagram comprising the drying path of a polymer-fullerene (1:0.8) solution (Details see section 3). b) Exemplary drying curve of a thin film with initially 3 wt.% solid fraction (Details see section 2).

Finally, it is important to investigate the systematic impact of different drying conditions on the blend film structure. If parameters such as drying temperature and drying gas velocity (gas phase mass transfer coefficient) are suitable for generating different film structures, the process-structure-property

relationship of solar cell devices will be investigated. Therefore suitable measurement techniques for the determination of the molecular, nanometer and micrometer scale structure have to be chosen or developed. The comparison with solar cell devices requires the elaboration of a solar cell fabrication process within the experimental setup of controlled drying kinetics.